THE JOURNAL OF BIOLOGICAL CHEMISTRY VOL. 290, NO. 40, pp. 24152–24165, October 2, 2015

ATP-binding Cassette Transporter A7 (ABCA7) Loss of Function Alters Alzheimer Amyloid Processing*

Received for publication, March 27, 2015, and in revised form, July 30, 2015 Published, JBC Papers in Press, August 10, 2015, DOI 10.1074/jbc.M115.655076

Kanayo Satoh[‡1], **Sumiko Abe-Dohmae**[§], **Shinji Yokoyama**[¶], **Peter St George-Hyslop**[‡‖**], **and Paul E. Fraser**[‡‖]

From the [‡]*Tanz Centre for Research in Neurodegenerative Diseases, University of Toronto, Toronto, Ontario M5T 2S8, Canada,* [§]*Biochemistry, Nagoya City University Graduate School of Medical Sciences, Nagoya 467-8601, Japan,* [¶]*Nutritional Health Science Research Center, Chubu University, Matsumoto-cho 1200, Kasugai 487-8501, Japan,* [‖]*Departments of Medicine (Neurology) and Medical Biophysics, University of Toronto, Toronto, Ontario M5G 1L7, Canada, and* **Cambridge Institute for Medical Research, University of Cambridge, Cambridge CB2 0XY, United Kingdom*

Background: The ATP-binding cassette transporter A7 (ABCA7) is a risk factor for sporadic Alzheimer disease (AD).
Results: Loss of ABCA7 promoted Aβ processing and pathology in cell culture and AD mouse models.
Conclusion: Altered ABCA7 function may contribute to AD by impacting Aβ production in addition to clearance.
Significance: AD-related risk factors may contribute to disease progression through multiple pathways.

The ATP-binding cassette transporter A7 (ABCA7) has been identified as a susceptibility factor of late onset Alzheimer disease in genome-wide association studies. ABCA7 has been shown to mediate phagocytosis and affect membrane trafficking. The current study examined the impact of ABCA7 loss of function on amyloid precursor protein (APP) processing and generation of amyloid-β (Aβ). Suppression of endogenous ABCA7 in several different cell lines resulted in increased β-secretase cleavage and elevated Aβ. ABCA7 knock-out mice displayed an increased production of endogenous murine amyloid Aβ42 species. Crossing ABCA7-deficient animals to an APP transgenic model resulted in significant increases in the soluble Aβ as compared with mice expressing normal levels of ABCA7. Only modest changes in the amount of insoluble Aβ and amyloid plaque densities were observed once the amyloid pathology was well developed, whereas Aβ deposition was enhanced in younger animals. *In vitro* studies indicated a more rapid endocytosis of APP in ABCA7 knock-out cells that is mechanistically consistent with the increased Aβ production. These *in vitro* and *in vivo* findings indicate a direct role of ABCA7 in amyloid processing that may be associated with its primary biological function to regulate endocytic pathways. Several potential loss-of-function ABCA7 mutations and deletions linked to Alzheimer disease that in some instances have a greater impact than apoE allelic variants have recently been identified. A reduction in ABCA7 expression or loss of function would be predicted to increase amyloid production and that may be a contributing factor in the associated Alzheimer disease susceptibility.

Genome-wide association studies have identified the ATP-binding cassette transporter A7 (*ABCA7*)[2] as a susceptibility locus for late onset Alzheimer disease (LOAD) (1, 2). The single nucleotide polymorphisms (SNPs) associated with LOAD are distributed in various domains of the *ABCA7* gene and include intronic SNPs and a coding sequence causing G1527A substitution. Studies have identified loci in different clusters, suggesting multiple sites within the *ABCA7* gene associated with increased risk for AD (3). However, there is no indication that individuals with at-risk alleles display any differences in ABCA7 expression.

ABCA7 is a member of the ATP-binding cassette transporter family largely involved in lipid transport and homeostasis (4). Its highly homologous member ABCA1 has also been linked to LOAD through cholesterol and processing of the amyloid precursor protein (5–7). Overexpression of ABCA7 resulted in a significant decrease in amyloid-β (Aβ) processing (8). It was therefore suggested that ABCA7 directly impacts amyloid pathology by altering APP trafficking and substrate availability.

Human ABCA7 overexpressed in HEK293 cells mediated generation of HDL containing less cholesterol as compared with ABCA1 (9, 10). Mouse ABCA7 under the same conditions generated HDL almost exclusively composed of phospholipid (11). However, loss or reduction of ABCA7 demonstrated no change in cell lipid release, indicating that it is unlikely to be redundant with ABCA1 in HDL biogenesis (12–14). Transcription of ABCA7 is regulated by sterol regulatory element/sterol regulatory element-binding protein in an opposite direction to the liver X receptor-mediated regulation of ABCA1, suggesting that it is unlikely to mediate cell cholesterol release (14). Subsequent studies demonstrated that endogenous ABCA7 is primarily associated with endocytic pathways, including phagocytosis (14). Thus, endogenous ABCA7 is speculated to link sterol

* This work was supported by Canadian Institute of Health Research Grant MOP-115056 (to P. E. F.), the Ontario Alzheimer's Society, the Ontario Research Fund, Japan Society for the Promotion of Science KAKENHI Grants 21591164 and 25461375, the Japan Health Sciences Foundation, and the Ministry of Education, Culture, Sports, Science and Technology-supported program for the Strategic Research Foundation at Private Universities (Japan). The authors declare no competing financial interests.
[1] To whom correspondence should be addressed: Tanz CRND, University of Toronto, 60 Leonard Ave., Toronto, Ontario M5T 2S8, Canada. E-mail: kanayo.sato@utoronto.ca.

[2] The abbreviations used are: ABCA7, ATP-binding cassette transporter A7; AD, Alzheimer disease; LOAD, late onset Alzheimer disease; APP, amyloid precursor protein; Aβ, amyloid-β; ABCA1, ATP-binding cassette transporter A1; sAPP, secreted APP; APP-FL, full-length APP; CTF, C-terminal fragment; APPSw, APP Swedish mutation; PICALM, phosphatidylinositol clathrin assembly lymphoid-myeloid leukemia; Tg, transgenic.

metabolism to host defense pathways rather than lipoprotein generation (15–17).

Similar studies found that ABCA7 suppression reduced clearance of apoptotic cell debris and that endogenous ABCA7 co-localized with LRP1 in stimulated macrophages (18). Exposure of apoptotic cells facilitated enrichment in cell surface ABCA7 and LRP1, and this was attenuated in ABCA7-hemizygous deficient mice (18). It is therefore conceivable that ABCA7 is linked to AD through a diminished ability to remove neuronal debris and/or amyloid aggregates. Our findings indicate that ABCA7 may also contribute to APP processing and Aβ production possibly by modulating LRP1 function. LRP1 associates with APP in the presence of a cytoplasmic adaptor protein, FE65, to internalize APP and produce Aβ in endosomal-lysosomal compartments (19, 20). The exact role of ABCA7 in LOAD is under debate, and it may contribute to Alzheimer pathology by altering Aβ production and/or clearance. The current study focused on ABCA7 loss of function and its involvement in amyloid processing in an effort to reconcile these two possible mechanisms.

Experimental Procedures

Antibodies—ABCA7 expression levels of cell and brain lysate were detected by Western blotting using rat monoclonal antibodies for human ABCA7 (KM3096) and mouse ABCA7 (KM3097). Samples were separated on 4–20% Mini-PROTEAN Tris-glycine extended precast gels (Bio-Rad). Anti-ABCA7 antibodies were provided by Kyowa Hakko Kirin Co. Ltd. Mouse monoclonal antibody 6E10 (Covance) was used for the APP internalization assay, and rabbit polyclonal anti-EEA1 antibody (ab2900, Abcam), an early endosome marker, was used for endosome immunostaining.

Plasmids and RNAi—Full-length cDNAs for human *ABCA7* were cloned as described previously (21). ABCA7 cDNA within pEGFP-N3 was digested by EcoRI and subcloned into pcDNA3 (Life Technologies). The vector has an immediate early promoter of cytomegalovirus promoter for expression of cDNA. Three sets of Stealth RNAi™ small interfering RNA (siRNA) duplexes specific for *ABCA7* (5′-GGAACCUGUCUGACUUCC UGGUCAA-3′, 5′-CCGCACUGCUGGUU-CUGGUGCUCAA-3′, and 5′-CGGAUCUUGAA-ACAGGUCUUCCUUA-3′) were designed and purchased from Life Technologies. High GC duplex was used as a negative control.

Cell Culture and Transfection—HEK293, KNS-42, SH-SY5Y, and HeLa cells were maintained in Dulbecco's modified Eagle's medium (DMEM; Life Technologies) supplemented with 10% (v/v) fetal calf serum in a humidified incubator with 5% CO_2 at 37 °C. The cells were grown on 35-mm glass-bottomed dishes. cDNA and Stealth RNAi siRNAs were transfected with Lipofectamine LTX and PLUS Reagent (Life Technologies) according to the manufacturer's protocols. Cells were examined 48 h after transfection. For primary cells, ABCA7-deficient mice (ABCA7−/−) were cross-bred with TgCRND8 (ABCA7+/+) mice. Primary cultures were prepared from brain of either embryonic 16-day-old (cortical neurons) or postnatal 1-day-old (astrocytes and microglia) mice according to the method of Cole and de Vellis (22), and mixed glial cells were cultured as described previously (23, 24). After 20–24 days of culturing, microglia were harvested by mild trypsinization (25). Briefly, cortical neurons were maintained in Neurobasal medium (Life Technologies) supplemented with B27 (Life Technologies), GlutaMAX (Life Technologies), sodium pyruvate (Life Technologies), and penicillin/streptomycin (Life Technologies) by a twice weekly half-volume medium change. Astrocyte and microglia cultures were maintained in DMEM supplemented with GlutaMAX, minimum essential medium amino acids (Life Technologies), minimum essential medium vitamin solution (pH 7.2; Life Technologies), and 10% (v/v) fetal calf serum by a twice weekly complete medium change in a humidified incubator with 5% CO_2 at 37 °C. All experiments were performed according to the Canadian Council on Animal Care guidelines.

Preparation of Cell and Brain Lysates—HEK293, KNS-42, SH-SY5Y, and HeLa cells and mouse primary microglia were cultivated and solubilized with radioimmune precipitation assay buffer (150 mM NaCl, 50 mM Tris, 1% Triton X-100, 0.5% deoxycholate, 0.1% SDS, 1 mM EDTA, pH 7.6). Protein quantitation was performed using the method of Bradford (64). Mouse hemibrain or dissected samples were homogenized in a buffered sucrose solution (20 mM HEPES, pH 7.4, 0.25 M sucrose, 1 mM EDTA, 1 mM EGTA) and a protease inhibitor mixture followed by 1.0% Nonidet P-40 lysis buffer to examine the endogenous APP/Aβ level. To isolate soluble/insoluble Aβ, hemibrain or dissected samples were homogenized in a buffered sucrose solution followed by either a mixture of 0.4% diethylamine and 100 mM NaCl for soluble Aβ or cold formic acid for the isolation of total Aβ. After neutralization, samples were diluted and analyzed for Aβ40 and Aβ42 levels.

APP Processing Analysis—Approximately 48 h after transfection, conditioned medium was collected and analyzed for Aβ40, Aβ42, secreted APP (sAPP) β/Sw, and sAPPβ/WT levels using commercially available ELISA kits (human Aβ40 and human Aβ42 from Life Technologies and mouse Aβ40, mouse Aβ42, human sAPPβ/Sw, and human sAPPβ/WT from IBL International). Levels of full-length APP and C-terminal fragment of APP in cell lysate and brain lysate were analyzed by Western blotting using the monoclonal antibody C1/6.1 as described previously (26). The conditioned medium or brain lysate was used to analyze secreted APPs, sAPPβ/Sw, sAPPβ/WT, and Aβ levels by Western blotting using monoclonal antibody 22C11 for secreted APPs (Chemicon), monoclonal antibody 6A1 for human sAPPβ/Sw (IBL International), polyclonal antibody for human sAPPβ/WT (IBL International), and monoclonal antibody 6E10 for sAPPα and Aβ (Signet/Covance).

Knock-out and Transgenic Mice—The TgCRND8 transgenic mice express APP695 on a prion cos-tet vector on a C57BL/6/C3H mixed background as described previously (27). The ABCA7 knock-out mice were generated as described previously (28) and maintained on a C57BL/6 background. An equal mix of age-matched male and female mice was examined in this investigation. The TgCRND8-ABCA7+/+ and TgCRND8-ABCA7−/− crosses were maintained on the same C57BL/6/C3H mixed background to avoid any background-related variations in APP expression and amyloid pathology.

Analysis of Aβ Plaque Densities—Animals were perfused, and brains were fixed in 4% paraformaldehyde and prepared for immunostaining as described previously (29). Plaques were

identified using an HRP-conjugated primary Aβ-specific antibody (6E10-HRP, Signet) and visualized with 3,3′-diaminobenzidine following pretreatment with 70% formic acid. Dense and diffuse plaque stainings were assessed by measuring the amyloid-positive area over total area as described previously (30). Briefly, immunostained sections (5 μm) were scanned with Mirax Scan (Zeiss) and assessed using ImageScope (Aperio). Slides were scanned using the Mirax Scan v.1.11 software and Zeiss Mirax Slide Scanner at 20× magnification with a Zeiss 20×/0.8 objective lens and a Marlin F146-C charge-coupled device camera. The rendered digital images were analyzed using the color deconvolution algorithm in the ImageScope software as described previously (31). RGB values were determined for both the applied hematoxylin and 3,3′-diaminobenzidine stains. 3,3′-Diaminobenzidine was chosen as the positive color channel for identifying and quantifying Aβ-stained plaques within different areas of the brain (cortex and hippocampus). Furthermore, recognition and measurement of dense and diffuse plaque stained areas were achieved by setting the threshold values of color intensity. The strong positive threshold was set to 80, correlating with dense staining; the medium positive threshold was set to 160, correlating with medium/diffuse staining; and the weak positive threshold was set to 0. In this way, the amyloid-positive area as well as the intensity of Aβ staining was quantified in different brain regions, allowing for quick, objective comparison between brains from different animals.

APP Endocytosis and ABCA7/Endosome Localization—The primary microglia from P1 C57BL/6 or ABCA7 knock-out mice were cultured for 3 weeks on 35-mm dishes (Nunclon), then washed with cold PBS, and incubated at 4 °C with 6E10 antibody (1:200 in PBS) for 30 min to label surface APP. Cells were carefully rinsed with ice-cold PBS and incubated at 37 °C for 0, 5, 10, and 20 min to permit internalization. Cells were fixed in 4% paraformaldehyde in PBS for 10 min at room temperature, permeabilized in 0.1% Triton X-100, washed in 0.1% Tween 20 in PBS, and blocked in 5% normal goat serum in PBS-Tween 20. Cells were then incubated with anti-ABCA7 antibody (KM3097) or anti-EEA1 primary antibody, washed, and then incubated with goat Cy3-conjugated anti-mouse IgG and goat FITC-conjugated anti-rat or -rabbit IgG (Jackson ImmunoResearch Laboratories). Cells were mounted with fluorescent mounting medium (Dako) or Prolong Gold antifade reagent with DAPI (Life Technologies). Fluorescence images were observed using an Axioplan 2 imaging microscope (Zeiss) and AxioVision software (Zeiss) equipped with a laser-scanning confocal (LSM-510, Zeiss) or an AxioObserverZ1 inverted microscope (Zeiss) equipped with a spinning disk confocal scanner (CSU-XI, Yokogawa), an Axiocam 506 camera (Zeiss), an Evolve 512 electron-multiplying charge-coupled device camera (Photometrics), and a 63× (oil; numerical aperture, 1.40) objective lens (Zeiss). Imaging data were analyzed using Volocity version 6.3.0 (PerkinElmer Life Sciences).

Statistical Analysis—All data were analyzed by Prism 5 (GraphPad Software), Igor Pro 6.02 (WaveMetrics), or Excel (Microsoft) using either a two-tailed Student's *t* test or Tukey-Kramer test. Data were expressed as mean ± S.D. Differences were deemed significant at $p < 0.05$ (*), $p < 0.01$ (**), and $p < 0.001$(***).

Results

In Vitro Suppression of Endogenous ABCA7 and Aβ Generation—Endogenous ABCA7 in a number of different cell lines was examined using human-specific monoclonal anti-ABCA7 antibody (KM3096), which revealed variability in the level of expression. The neuroblastoma SH-SY5Y and HEK293 cells did not express any detectable ABCA7 (Fig. 1*A*). In contrast, HeLa cells expressed moderate levels of ABCA7, and higher levels were expressed in the glioma KNS-42 cells. All cell lines had equivalent levels of endogenous APP (Fig. 1*A*).

Transient overexpression of mouse ABCA7 was previously demonstrated to result in significant reductions in Aβ levels for cells co-expressing human APP (8). Our investigations of cells transfected with human ABCA7 and APP have supported the link to altered APP processing resulting in a significant decrease in secreted Aβ (data not shown). However, comparable studies examining lipid efflux suggest that the cellular effects of transfected ABCA7 do not reflect the function of the endogenous protein (16). Because of the potentially confounding issues associated with artificially high expression levels of ABCA7, the current study focused on loss-of-function conditions and the consequences these have for amyloid processing and deposition within the brain.

For knockdown studies, KNS-42 cells have the highest ABCA7 expression, but this line has low transfection efficiency, and despite repeated attempts, it was not possible to obtain sufficient knockdown of ABCA7. We therefore examined suppression of ABCA7 in HeLa cells using three independent siRNA duplex constructs. Endogenous HeLa ABCA7 was assessed with a human-specific monoclonal antibody. All three RNAi constructs were found to virtually eliminate expression when compared with a negative control or untransfected cells (Fig. 1*B*). Examination of endogenous APP processing in the HeLa cells revealed a small but detectable increase in the sAPPβ species as determined by immunoblotting (Fig. 1*C*). This effect was confirmed by ELISA quantification of the HeLa endogenous sAPPβ/WT (Fig. 1*C*). To ascertain the effects on Aβ generation, cells were transfected with APPSw with and without ABCA7 knockdown. The levels of full-length APP (APP-FL) and C-terminal fragments (APP-CTFs) were not significantly different (Fig. 1*D*). Total levels of secreted APP (sAPP) were not significantly altered by ABCA7 suppression (Fig. 1*E*). An ELISA assessment confirmed the elevated levels of secreted APPβ/Sw (Fig. 1*F*). In addition to the increase in β-cleavage, elevations in Aβ40 and Aβ42 peptides for cells lacking endogenous ABCA7 expression were seen as compared with the negative control or APP-only expression (Fig. 1, *G* and *H*). Greater variation was observed for cells transfected with the RNAi control as compared with untransfected cells, which reduced the statistical significance of the ABCA7 knockdown cells. This may reflect the low levels of endogenous HeLa ABCA7, which reduces the impact of ABCA7 loss on APP processing and Aβ production. The reduction is therefore modest, but cumulatively, these observations are consistent with a direct action of ABCA7 on

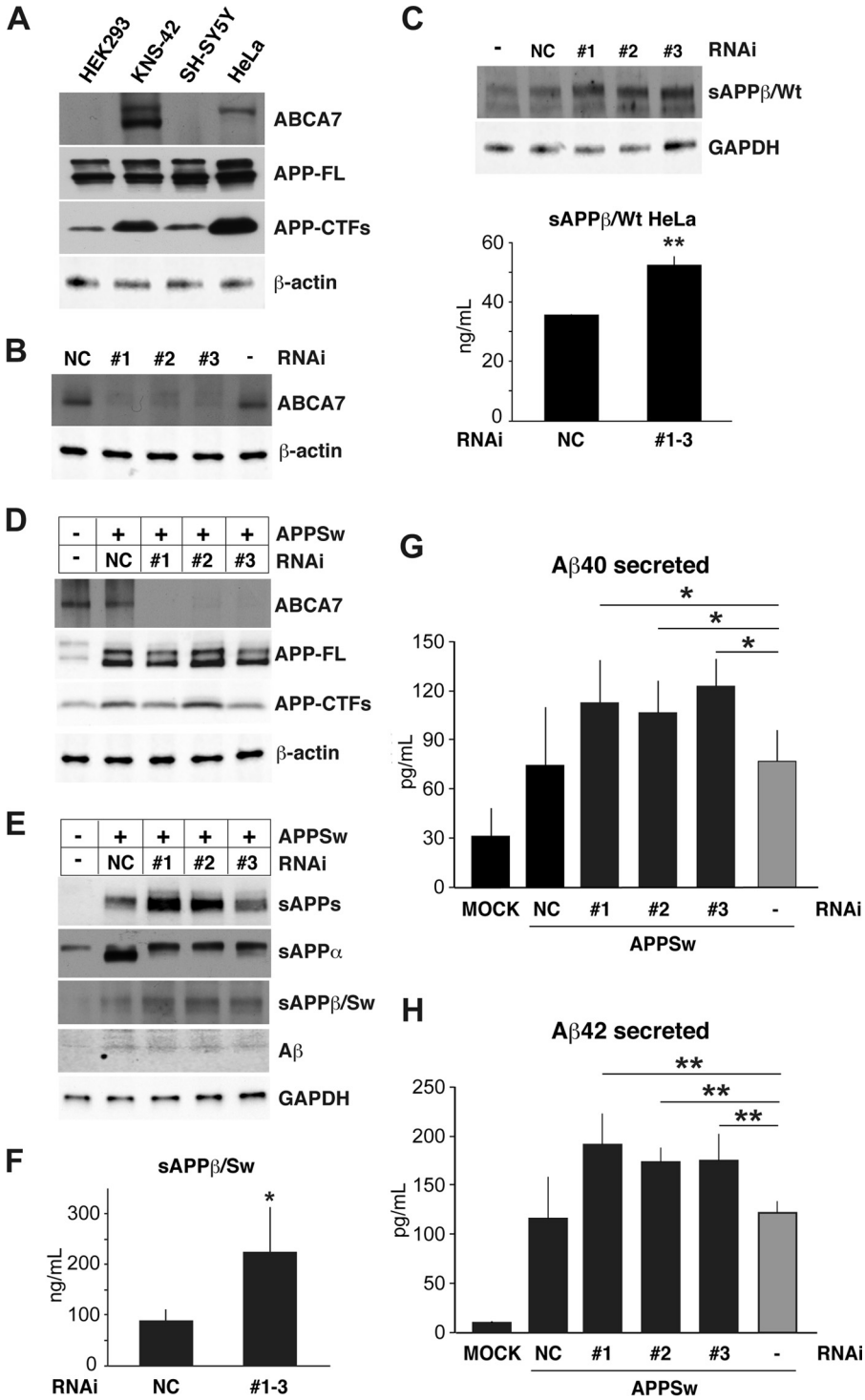

FIGURE 1. **ABCA7 knockdown effects on APP processing and Aβ production in HeLa cells.** *A*, Western blot analysis of endogenous ABCA7 in different cell lines indicated the highest levels in the glioma KNS-42 cells and modest levels in HeLa cells, whereas ABCA7 was undetectable in HEK293 and SH-SY5Y cells (15 μg of total protein/lane). Levels of full-length endogenous APP were comparable among the different cell lines, and increases in APP-CTF were observed in cells expressing ABCA7. *B*, suppression of endogenous ABCA7 in HeLa cells by three independent RNAi constructs (*#1–3*) as compared with a negative control (*NC*) was validated by Western blotting using a human-specific ABCA7 monoclonal antibody (15 μg of total protein/lane). *C*, effect of ABCA7 knockdown on endogenous APP as assessed by Western blotting revealed a modest increase in sAPPβ/WT. Quantification of sAPPβ/WT by ELISA confirmed the increased levels possibly due to preferential β-secretase cleavage in the absence of ABCA7. The data represent means $\pm$ S.D. (*error bars*) of six independent measurements. **, $p < 0.01$ by Student's *t* test. *D*, Western blotting of HeLa cells transiently transfected with APPSw with and without ABCA7 suppression revealed no detectable changes in APP-FL or APP-CTF. *E*, immunoblotting of HeLa cells transiently transfected with APPSw to examine total sAPP and the specific sAPPα and sAPPβ/Sw species demonstrated a slight increase in sAPPβ/Sw for cells with reduced ABCA7 levels. No immediately obvious differences were observed for total Aβ by Western blotting. *F*, ELISA analysis for sAPPβ/Sw confirmed the increased levels possibly due to preferential β-secretase cleavage in the absence of ABCA7. The data represent means $\pm$ S.D. (*error bars*) of four independent measurements. *, $p < 0.05$ by Student's *t* test. *G* and *H*, knockdown of endogenous ABCA7 was accompanied by significant increases in Aβ40 and particularly Aβ42 as compared with those transfected with APPSw alone as determined by ELISA. The data represent means $\pm$ S.D. (*error bars*) of eight independent measurements. *, $p < 0.05$; **, $p < 0.01$ as determined by Tukey-Kramer test.

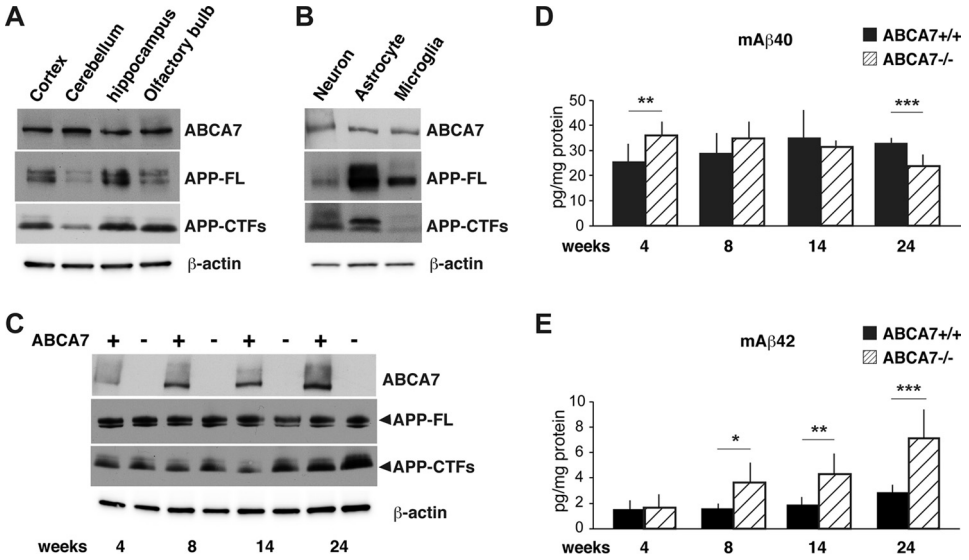

FIGURE 2. **ABCA7 knock-out increases endogenous murine Aβ42.** *A*, levels of endogenous ABCA7 in different regions of mouse brain examined with a murine-specific monoclonal antibody indicated no major variations in expression levels. Western blotting for APP-FL and -CTF did not reveal any correlations with ABCA7 within the same brain areas. *B*, immunoblotting of endogenous ABCA7 in primary cells from non-transgenic mice displayed comparable expression levels in all cell types, and no consistent changes in APP-FL or -CTF were observed. *C*, Western blot analysis for endogenous ABCA7, APP-FL and APP-CTF for wild-type (+) and ABCA7 knock-out (−) mice over the course of 4–24 weeks of age. Total brain lysates of wild-type ABCA7 and ABCA7 knock-out mice confirmed the expected absence in the knock-outs and a progressive increase in wild-type mice over the course of 4–24 weeks of age (40 μg of total protein/lane). No differences were observed in any of the APP species as a result of ABCA7 knockdown. *D* and *E*, ELISA analysis for endogenous murine Aβ40 indicated a decline in levels with age (*D*). ELISA analysis for endogenous murine Aβ42 revealed a significant elevation with age in animals lacking ABCA7 (ABCA7−/−) as compared with wild-type mice (ABCA7+/+) (*E*). The data represent means ± S.D. (*error bars*) of six to eight individual mice. *, $p < 0.05$; **, $p < 0.01$; ***, $p < 0.001$ by Student's *t* test.

APP processing leading to Aβ production possibly by modulating the efficiency of β-secretase cleavage.

Endogenous Murine Aβ42 Increases in ABCA7 Knock-outs—Loss of function was explored further in a physiological setting using an ABCA7 knock-out mouse model (28). Expression of ABCA7 in the wild-type mice was examined using murine-specific monoclonal antibodies, and comparable levels were found in all brain regions (Fig. 2*A*). Nearly identical levels of ABCA7 expression were observed in primary neurons and glia from wild-type mice (Fig. 2*B*). These findings indicate that ABCA7 is found throughout the brain and is expressed by all major cell types.

ABCA7 levels were also examined in total brain extracts from wild-type and knock-out animals over different time points after weaning until 6 months of age. The expected lack of ABCA7 was observed in the ABCA7 knock-out mice (ABCA7−/−), and a modest increase in ABCA7 levels was observed in wild-type mice (ABCA7+/+) from 4 to 24 weeks of age (Fig. 2*C*). No significant differences in APP-FL or APP-CTF were seen between ABCA7+/+ and ABCA7−/− mice at comparable ages (Fig. 2*C*). Quantification of endogenous mouse Aβ40 revealed a higher concentration in 4–8-week-old ABCA7−/− mice that gradually diminished to culminate in slightly lower levels than those of wild-type animals (ABCA7+/+) at 14–24 weeks of age (Fig. 2*D*). In contrast, a specific increase in Aβ42 during aging was observed with the loss of ABCA7. Endogenous murine Aβ42 was roughly equivalent in the 4-week-old animals, progressively increased in the ABCA7−/− mice, and was significantly higher than in ABCA7+/+ mice at 8–24 weeks of age (Fig. 2*E*). A comparison of genders indicated a slight elevation in Aβ42 levels in male ABCA7−/− mice (8.63 ± 1.62 pg/mg of protein) as compared with females (5.57 ± 1.79 pg/mg of protein), although these were not statistically significant ($n = 3$ in both groups). Total brain Aβ42 in the ABACA7+/+ mice was also slightly higher at 24 weeks of age, but this did not reach statistical significance when compared with younger mice (Fig. 2*E*). These findings, particularly the specific Aβ42 elevation, are consistent with ABCA7-mediated changes in both β- and γ-secretases.

Links between Aβ production and cholesterol have been extensively reported where high fat diets lead to increased amyloid processing (for a review see, Ref. 32). To determine whether changes in putative ABCA7-mediated cholesterol and lipid pathways had any impact on endogenous Aβ generation, ABCA7 knock-outs were compared with wild types that were placed on fat-enriched diets postweaning until 14 weeks of age. Expression of ABCA7 decreased slightly in the wild-type animals, which is consistent with the sterol regulatory element-binding protein 2 regulation and effects of sterols on ABCA7 (14). Substantial increases in APP-FL and APP-CTFs were observed for animals on a high fat diet (Fig. 3*A*). However, total brain Aβ40 and Aβ42 were nearly identical in the wild-type and knock-out mice under these conditions, and the differences in Aβ42 seen for animals on normal diet were eliminated (Fig. 3, *B* and *C*). The mice on a high fat diet were compared with the same animals on a normal diet that were used to determine the endogenous Aβ40 and Aβ42 levels (see Fig. 2). These observations indicate that increased cholesterol and lipid did not have an additive effect on amyloid processing in the ABCA7-ablated mice.

Loss of ABCA7 Increases Soluble Aβ in APP Transgenic Mice—The changes in endogenous mouse Aβ42 for mice lacking ABCA7 indicate that ABCA7 affects pathways related to secretase cleavages of APP. To examine these pathways in more

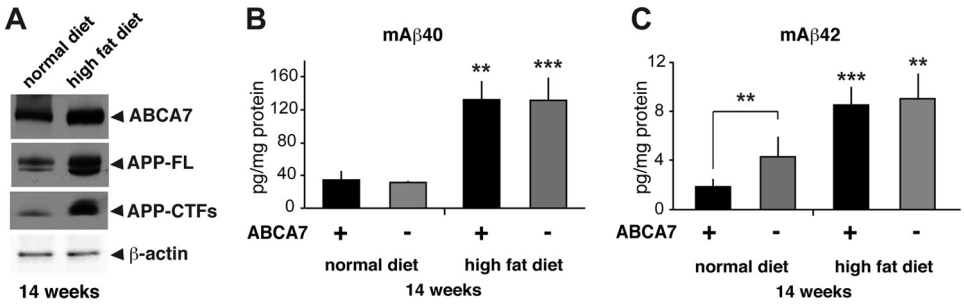

FIGURE 3. **APP expression in ABCA7 knock-out mice and effects of high fat diet.** *A*, Western blotting for wild-type mice on normal and high fat diets indicated no significant changes in ABCA7 levels, but an increase in APP-FL and APP-CTF was observed for animals on the high fat diet (40 μg of total protein/lane). *B* and *C*, levels of endogenous murine Aβ40 and Aβ42 in wild-type (+) and ABCA7 knock-out (−) mice at 14 weeks of age were increased in both groups, and the differences in Aβ42 were eliminated on the high fat diet. The Aβ40 and Aβ42 data shown for mice on the normal diet are from the same group of animals used to determine endogenous Aβ levels as shown in Fig. 2. The data represent means ± S.D. (*error bars*) of eight individual mice. **, $p < 0.01$; ***, $p < 0.001$, by Student's *t* test.

detail and determine the effects on amyloid pathology, ABCA7 knock-out mice were crossed with a mutant APP transgenic mouse model (TgCRND8). The TgCRND8 model has been widely used and is an aggressive model with AD-related amyloid plaques and oligomers forming within 3–4 months of age (27, 29). The TgCRND8-ABCA7−/− cross was compared with TgCRND8 on a wild-type ABCA7 background at 18 weeks of age when extensive amyloid pathology is observed in this particular model. ABCA7 levels in TgCRND8 mice were comparable with non-transgenic animals, indicating that the APP transgene does not have any appreciable impact on ABCA7 expression (data not shown).

Western blotting for APP revealed the expected high levels of APP-FL, which were equivalent in both TgCRND8-ABCA7−/− and TgCRND8-ABCA7+/+ (Fig. 4*A*). However, a slight increase in APP-CTFα/β was observed in the TgCRND8-ABCA7−/− mice as compared with TgCRND8 alone. Secreted APPβ was also increased in TgCRND8-ABAC7−/− mice as determined by ELISA (Fig. 4*B*). A statistically significant elevation in soluble Aβ40 was observed in whole brain extracts from TgCRND8-ABCA7−/− mice (Fig. 4, *C*). The soluble Aβ42 and insoluble Aβ40 or Aβ42 tended to be higher in the ABCA7-deficient mice, but these values did not achieve statistical significance (Fig. 4, *C* and *D*). These findings indicate that the loss of ABCA7 has a direct impact by altering APP processing, leading to increased Aβ production similar to that observed for endogenous mouse amyloid.

Assessment of soluble and insoluble Aβ was conducted in specific brain regions associated with AD-related pathology to determine whether similar trends were observed as compared with whole brain extracts. Soluble Aβ40 and Aβ42 were found to be the highest in the cortex, and significant increases in both species were observed in the APP transgenic mice (TgCRND8) on the ABCA7 knock-out background (Fig. 5, *A* and *C*). Similar trends were observed for soluble Aβ40 and Aβ42 in the hippocampus, cerebellum, and olfactory bulb of TgCRND8-ABCA7−/− mice as compared with TgCRND8-ABCA7+/+ animals (Fig. 5, *A* and *C*). The most pronounced changes in soluble Aβ42 were in the cortex and olfactory bulb where an ~4-fold increase was detected (Fig. 5*C*). The olfactory bulb is an area of extensive pathology in the TgCRND8 model due to the prion cos-tet promoter that drives high expression in this region (33). In contrast, insoluble Aβ40 and Aβ42 in the cortex and hippocampus did not exhibit statistically significant differences between TgCRND8-ABCA7−/− and TgCRND8-ABCA7+/+ mice (Fig. 5, *B* and *D*). In the olfactory bulb, increased amounts of insoluble Aβ were found in the transgenic mice lacking ABCA7, likely reflecting the high level of APP expression and Aβ production. No significant differences in soluble Aβ levels were observed between males and females in this study. These findings are in keeping with the whole brain extracts and demonstrated that Aβ generation is increased and accumulates as plaques.

Amyloid Plaque Density in ABCA7 Knock-outs Crossed with APP Transgenic Mouse Model—Amyloid deposition in the mouse models at 18 weeks of age was examined by immunohistology to quantify plaque density. Serial sections from successive regions of the brain were stained for total Aβ, and typical amyloid plaques were observed in the cortex and hippocampus of the APP transgenic mice on the ABCA7 wild-type and knock-out backgrounds (Fig. 6, *A* and *B*). Image analysis of dense and diffuse plaque areas was conducted with sampling over the entire cortex and hippocampus. Quantification of the staining revealed a statistically significant increase in TgCRND8-ABCA7−/− mice in dense core plaques area, but no detectable change in the diffuse plaque area was observed (Fig. 6*C*). The total number of plaques, as opposed to average size, showed a slight trend to higher amounts in the ABCA7 knock-out mice, but this did not achieve statistical significance when compared with the TgCRND8 on an ABCA7 wild-type background (Fig. 6*D*). The increase in the area of dense plaques is likely a reflection of the increased production of Aβ in the TgCRND8-ABCA7−/− mice.

Amyloid Deposition at Early Stages of Pathology Development—Given the observed elevations in soluble Aβ displayed by the TgCRND8-ABCA7−/− mice, it could have been expected that this would translate into increased plaque loads for these animals as compared with TgCRND8 transgenic mice on an ABCA7+/+ background. A likely explanation is that aggregation and deposition of the insoluble Aβ have plateaued in the older animals (18 weeks), and to investigate this possibility in more detail, comparable mice were examined at 10 weeks of age. Previous studies have indicated that at ~10 weeks of age the TgCRND8 mouse model undergoes a transition where the total amount of Aβ42 generated by the transgenic mice

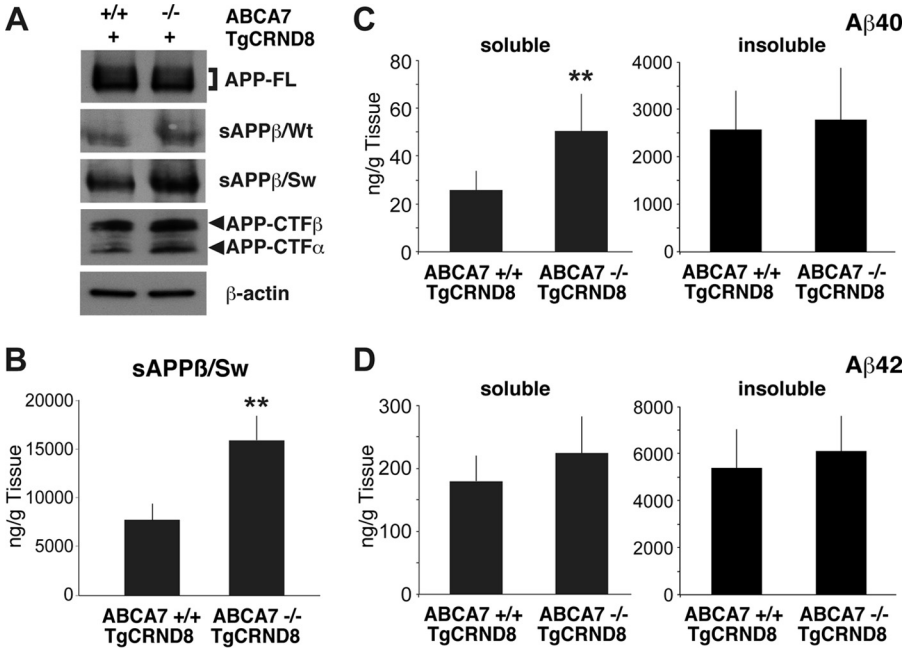

FIGURE 4. **Amyloid processing in APP transgenic mice lacking ABCA7.** *A*, the levels of APP-FL and -CTFs in TgCRND8 mice (18 weeks) and ABCA7 knock-out and TgCRND8 double transgenic mice (TgCRND8-ABCA7−/−; 18 weeks). *B*, total brain sAPPβ/Sw levels were increased by ~60% in the APP transgenic mice on the ABCA7 knock-out background as determined by ELISA. The data represent means ± S.D. (*error bars*) of six independent measurements. **, $p < 0.01$ by Student's *t* test. *C* and *D*, soluble Aβ40 from total brain lysates was significantly increased in ABCA7 knock-out mice, whereas no changes in the insoluble form were observed (*C*). Comparable ELISA analysis indicated an increase in soluble Aβ42 and the plaque-associated insoluble species in the mice lacking ABCA7 but no significant differences (*D*). The data represent means ± S.D. (*error bars*) of 10–12 individual mice. *, $p < 0.01$ by Student's *t* test.

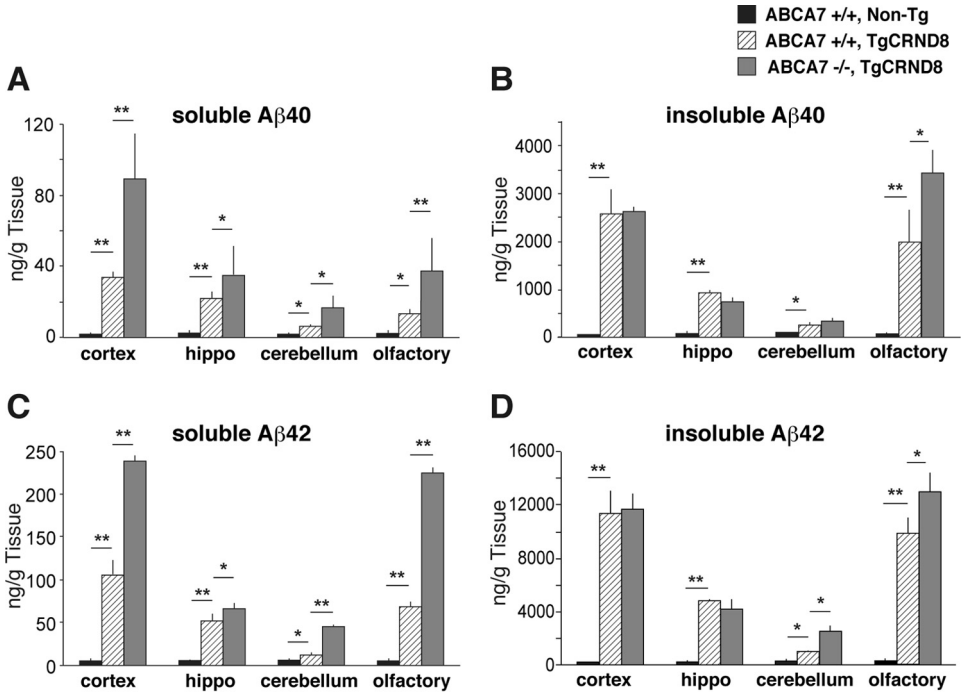

FIGURE 5. **Loss of ABCA7 increases soluble Aβ in all brain regions.** The levels of soluble and insoluble Aβ40 and Aβ42 were assessed in cerebral cortex (*cortex*), hippocampus (*hippo*), cerebellum, and the olfactory bulb (*olfactory*) for mice at 18 weeks of age by ELISA. The absolute amount of Aβ40 or Aβ42 varied in the different brain areas, but a consistent increase in the soluble species was observed. Similar to total brain extracts, the quantity of insoluble Aβ40 and Aβ42 was generally comparable between APP transgenic mice expressing endogenous ABCA7 and those on the knock-out background. However, increases in the insoluble Aβ40 and Aβ42 were observed in the olfactory bulb. The data represent means ± S.D. (*error bars*) of four individual mice. *, $p < 0.05$; **, $p < 0.01$ as determined by Tukey-Kramer test.

increases ~3-fold, and this is closely followed by the appearance of amyloid plaques (27).

Western blotting for APP indicated similar levels in TgCRND8 mice on both the ABCA7 wild-type and knock-out backgrounds and models elevations in the β-secretase-cleaved protein (Fig. 7*A*). The increase in the secreted APPβ fragments was confirmed by ELISA, which is consistent with the observations in the older animals (Fig. 7*B*). As expected, quantification

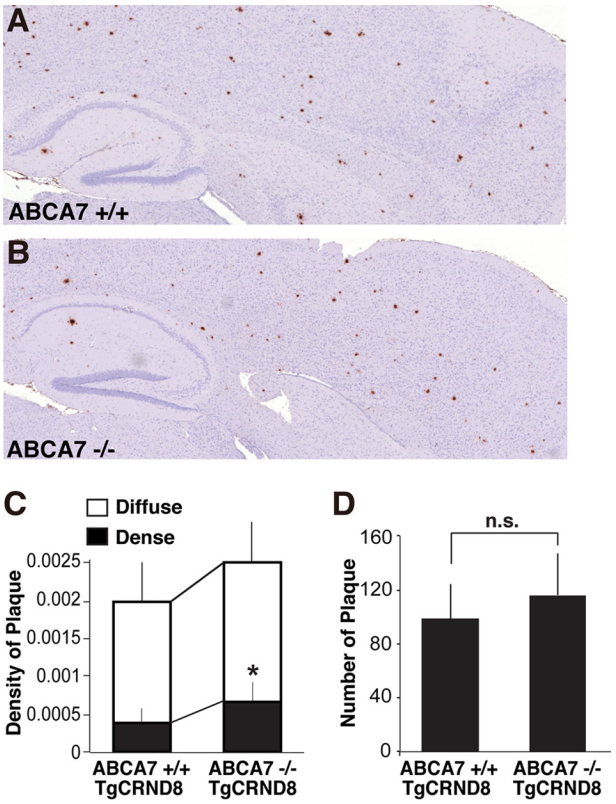

FIGURE 6. **Amyloid plaque density in APP transgenic mice lacking ABCA7.** Immunohistochemistry for total amyloid in APP transgenic mice (TgCRND8) on wild-type (+/+) and ablated ABCA7 (−/−) backgrounds. Representative images of diffuse and dense plaques in the cortex and hippocampus in TgCRND8 APP transgenic mice (*A*) and TgCRND8 mice-deficient for ABCA7 (*B*) are shown. Amyloid plaques were quantified in scanned slides by deconvolution image analysis algorithms (ImageScope). *C*, the total area of dense plaques was found to be higher in the APP transgenic mice lacking ABCA7, but no significant differences were observed for diffuse plaques. *D*, total plaque numbers were not significantly different in the two mouse models at 18 weeks of age. The data represent means ± S.D. (*error bars*) of six individual mice. *, $p < 0.05$; *n.s.*, not significant by Student's *t* test.

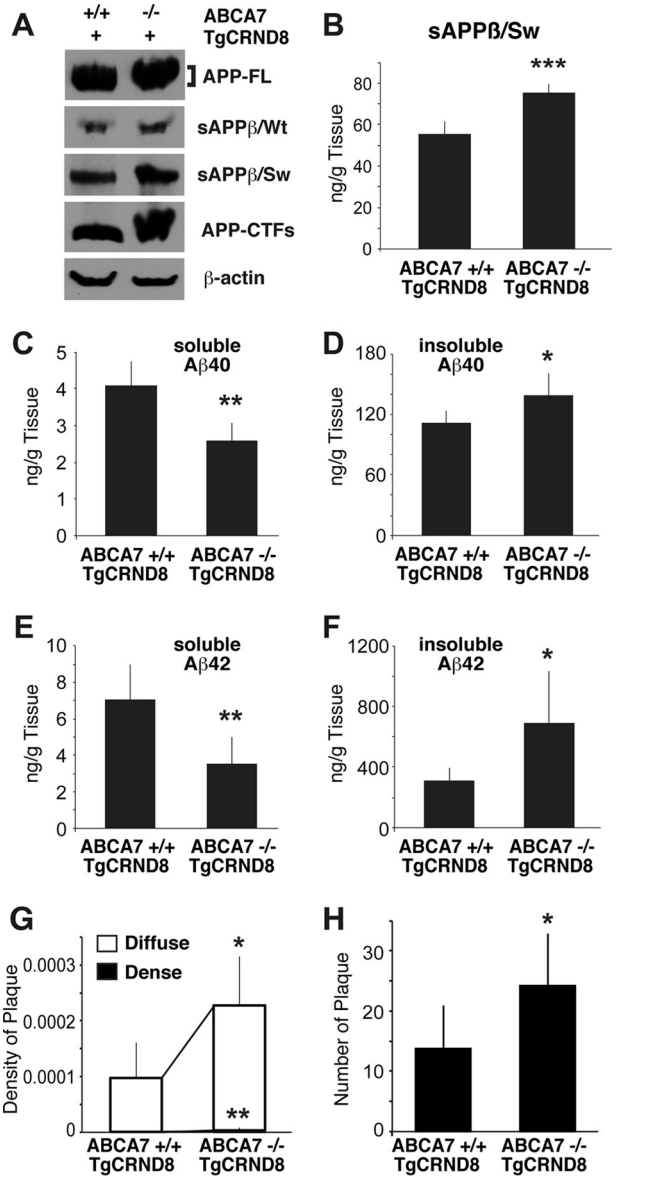

FIGURE 7. **Amyloid plaque density during early stages of pathology.** Quantitative analyses of APP species and Aβ levels in 10-week-old APP transgenic mice (TgCRND8) on an ABCA7 knock-out (−/−) or wild-type (ABCA7+/+) background. *A*, Western blotting of total brain extracts for APP-FL, β-secretase-cleaved secreted APP for the endogenous mouse protein (sAPPβ/WT) and transgenic protein (sAPPβ/Sw), and APP-CTFs. *B*, increased β-cleavage of transgenic APP in ABCA7 knock-out mice was confirmed by ELISA. Total Aβ levels were reduced as compared with 18-week-old mice, soluble Aβ40 was found to be lower in mice on the ABCA7−/− background (*C*), and insoluble Aβ40 was elevated in the same animals (*D*). Soluble Aβ42 was also decreased (*E*), and a comparable increase in insoluble deposited Aβ42 in ABCA7 knock-out animals (*F*) was seen. *G*, image analysis of Aβ immunohistochemistry indicated a substantial increase in the density of diffuse plaques and detection of dense plaques in APP transgenic mice lacking ABCA7. *H*, increases in the total number of plaques were also observed in ABCA7−/− mice. The data represent means ± S.D. (*error bars*) of six to 14 individual mice. *, $p < 0.05$; **, $p < 0.01$; ***, $p < 0.001$ by Student's *t* test.

of the Aβ in whole brain extracts indicated that the levels were lower in the 10-week-old animals as compared with those at 18 weeks of age. However, soluble Aβ40 and Aβ42 were both lower in the TgCRND8-ABCA7−/− animals as compared with those expressing normal levels of ABCA7 (Fig. 7, *C* and *E*). In contrast, insoluble Aβ40 and particularly Aβ42 were significantly higher in the TgCRND8 transgenic mice lacking ABCA7 (Fig. 7, *D* and *F*). The level of insoluble Aβ42 in the TgCRND8-ABCA7+/+ animals is consistent with previous reports where levels are ~300 ng/g of tissue (27). Transgenic mice lacking ABCA7 display greater than 600 ng/g insoluble Aβ42 (Fig. 7*F*). Immunohistochemistry for Aβ was performed on serial sections from both groups of mice, and image analysis revealed a substantial increase in the density of both diffuse and dense plaques in the ABCA7 knock-out mice, which is consistent with the observed elevations in the insoluble Aβ (Fig. 7*G*). In addition, increases in the total number of cortical and hippocampal plaques were found in TgCRND8-ABCA7−/− animals (Fig. 7*H*). The higher amounts of soluble Aβ in the older animals indicated that ABCA7 loss of function results in enhanced APP cleavage and the generation of Aβ peptides but not increased amyloid deposition. At the earlier 10-week stage, it appeared that the increased Aβ42 was aggregating rapidly and accumulating as amyloid plaques, which would account for the reduction in the soluble peptide. However, we cannot rule out the possibility that loss of ABCA7 in these animals may also have an impact on amyloid clearance.

APP Endocytosis Is Enhanced in ABCA7 Knock-outs—To explore potential mechanisms by which ABCA7 contributes to

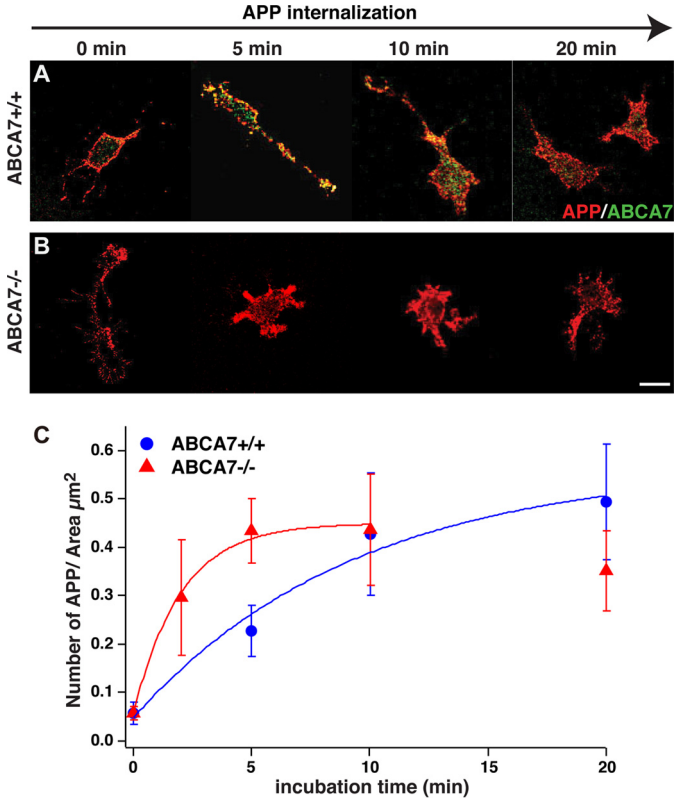

FIGURE 8. **Endocytosis of endogenous APP in ABCA7 knock-out cells.** Primary microglia cells from WT and ABCA7 knock-out mice were used to examine the rates of endocytosis for endogenous APP. Cell surface APP was labeled with 6E10 antibodies (*red*), and internalization was examined at 0, 5, 10, and 20 min. After fixation, cells were probed for endogenous ABCA7 (*green*). Cells expressing endogenous ABAC7 (*ABCA7*+/+) (*A*) displayed slower APP uptake of 15–20 min as compared with cells lacking ABAC7 (*ABCA7*−/−) (*B*), which exhibited APP endocytosis within the first 5 min of incubation. The *scale bar* represents 10 μm. *C*, quantitative analyses of APP internalization. The number of intracellular APPs was detected at each time point and divided by the area of the cells with Volocity. Data were fitted with exponential equation $Y = y_0 + A \times \exp(-1/\text{Tau} \times X)$. y_0 of WT and knock-out (KO) are 0.56891 ± 0.13 and 0.44988 ± 0.0207, *A* of WT and KO are −0.52098 ± 0.129 and −0.39347 ± 0.0287, and 1/Tau of WT and KO are 0.10604 ± 0.0607 and 0.5003 ± 0.0969, respectively (means ± S.D.). The data represent means ± S.D. (*error bars*). n = 13–24 in each group.

amyloid processing, the effects of loss of function on APP endocytosis were investigated. Primary microglia were isolated from wild-type and ABCA7 knock-out animals, and endogenous cell surface APP was labeled with monoclonal antibodies directed to the extracellular domain when cells were incubated at 4 °C (Fig. 8). Microglia were selected for this study as they express reasonable levels of both ABCA7 and APP (see Fig. 2) and have a morphology that makes them amenable to intracellular trafficking. Endocytosis was activated by bringing the cells to 37 °C, and internalization of the APP was monitored at different time points. After a 5-min incubation, the majority of the APP in wild-type cells was found at the surface and co-localized to some extent with plasma membrane ABCA7 (Fig. 8*A*). Some APP was internalized after 10 min, and progressively more cytoplasmic staining was observed at 20 min postincubation. In contrast, cells lacking ABCA7 exhibited a significant amount of intracellular APP after only 5 min of incubation (Fig. 8*B*). After 10 min, the majority of the endogenous APP was internalized, and similar staining was observed with longer incubations. Quantitative analysis revealed that the velocity of APP internalization during the first 5 min for ABCA7−/− cells was significantly more rapid than the uptake observed in wild-type cells (Fig. 8*C*). It has been shown previously that APP is internalized over a short time frame of 15 min or less (34). To examine the internalized APP in more detail, cells were double labeled with the endosomal marker EEA1, which showed considerable overlap with APP as expected (Fig. 9*A*). In ABCA7 knock-out cells, a greater degree of co-localization of APP and endosomes was observed, which is consistent with the accelerated uptake upon loss of ABCA7 (Fig. 9*B*). Quantification of the immunofluorescence after 5 min of endocytosis revealed significant differences in the overlap of EEA1 and APP in ABCA7−/− cells as compared with wild type as a function of total endosomal staining or total APP (Fig. 9, *C* and *D*). These differences were not due to variations in the amounts of EEA1 or APP levels as these were observed to be the same in ABCA7−/− and wild-type cells (Fig. 9, *E* and *F*). Cumulatively, these findings indicate that the loss of ABAC7 results in a rapid uptake of APP to endosomal compartments, which would account for the increased Aβ production seen both *in vitro* and *in vivo*.

Discussion

The identification of *ABCA7* as a susceptibility locus in recent genetic analyses has raised questions on how it may contribute to AD-related pathology and disease pathways. Our investigation examined the effects of ABCA7 on APP processing and Aβ deposition as one of the early key events in AD. These *in vitro* and *in vivo* studies revealed that ABCA7 loss of function significantly increased APP proteolysis and Aβ production. It is possible that changes in ABCA7 expression and/or activity may confer susceptibility through these aspects of the amyloid pathway. This would be consistent with recent studies that have demonstrated ABCA7 loss-of-function mutants and their association with increased risk for AD (35). In addition, changes in DNA methylation of several AD-related loci, including *ABCA7*, that correlated with amyloid load and neurofibrillary tangle density have been observed (36).

Knockdown of endogenous ABCA7 in HeLa cells resulted in an increase in sAPPβ processing of the endogenous protein indicative of increased amyloidogenic cleavage. This is in contrast to similar knockdown studies of various LOAD-related genes (*e.g. BIN1*, *Clustrin*, and *CD33*) where no effect on APP processing was observed, but *ABCA7* was not examined in this particular investigation (37). In the current study, loss of ABCA7 in cells overexpressing APPSw resulted in increased β-cleavage products and Aβ secretion. The Aβ40:Aβ42 ratios for the TgCRND8-ABCA7−/− (0.439 ± 0.173) and TgCRND8-ABCA7+/+ (0.533 ± 0.286) were comparable under these conditions, suggesting that there did not appear to be preferential γ-secretase cleavage at residue 42 *versus* 40. However, this was not the case for endogenous Aβ in ABCA7 knock-out mice. In brain tissue of wild-type mice, ABCA7 was found to be slightly elevated during aging, and its deletion resulted in a gradual increase in Aβ42 over the 6-month period investigated. The difference in brain Aβ42 levels between wild-type and ABAC7 knock-outs was eliminated when animals were put on high fat diets, which have been shown previously to

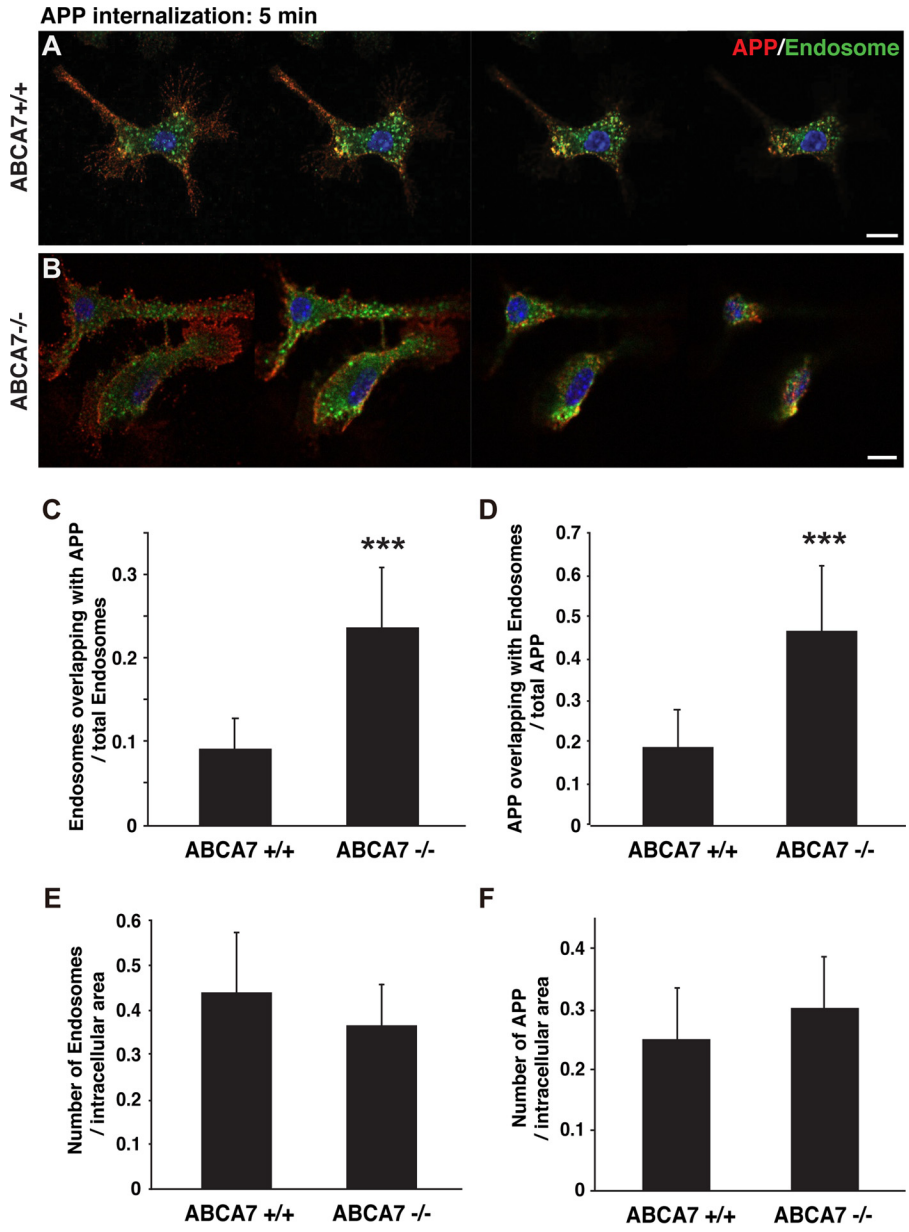

FIGURE 9. **Internalization of endogenous APP to endosomal compartments in ABCA7 knock-out cells.** Primary microglia cells from WT (*A*) and ABCA7 KO (*B*) mice were used to examine subcellular compartmentalization of APP and endosomes. After 5 min of APP endocytosis, more APP (*red*) overlapping with endosomes labeled with EEA1 antibodies (*green*) was observed in ABCA7 KO cells. The *scale bars* represent 10 μm. *C* and *D*, quantitative analyses of subcellular compartmentalization for APP and endosomes. The number of subcellular endosomes overlapping with APP after 5min of endocytosis was calculated and normalized with the total number of endosomes (*C*). The number of subcellular APPs overlapping with endosomes after 5 min of endocytosis was calculated and normalized with the total number of APPs (*D*). Endosomes overlapping with APPs and APPs overlapping with endosomes were significantly increased in ABCA7 KO cells as compared with wild-type cells. *E* and *F*, the numbers of subcellular endosomes and APPs in ABCA7 KO cells were comparable with those in WT cells. The data represent means ± S.D. (*error bars*). $n = 15$. ***, $p < 0.001$ by Student's *t* test.

up-regulate Aβ generation. Cumulatively, these findings indicate that ABCA7 has a direct impact on APP processing and γ-secretase. This may be mechanistically linked to the more rapid internalization and endosomal trafficking of APP that was observed for the ABCA7 knock-out cells.

It has been reported that mice lacking ABCA7 exhibit cognitive defects in the absence of any exogenous influences (38). A combination of behavioral tests was used to examine ABCA7 knock-out animals, and it was found that they had normal locomotion characteristics and fear conditioning-related memory and subtle differences in gender-specific impairments in some memory tasks. Only male knock-out mice exhibited impairments in novel object recognition that was not observed in female knock-out mice (38). There are likely to be several pathways involved in the ABCA7 knock-out cognitive deficit, but it is of interest to note the increased Aβ42, which may be a contributing factor as the animal ages. Additional studies, including the use of Aβ protease inhibitors, will be required to resolve these questions.

ABCA7 knock-out mice were crossed with an APP transgenic mouse, TgCRND8, to determine whether amyloid plaque levels and soluble Aβ were affected *in vivo*. We report here that examination of whole brain extracts revealed increases in soluble but not insoluble Aβ40 and Aβ42. This observation is of

note because many prior studies have supported a role for soluble Aβ oligomers in the synaptic and cognitive impairment during the early stages of AD (39–45). The conclusion that soluble Aβ species are the relevant moiety in ABCA7−/− mice is supported by plaque density quantification, which showed modest increases in the dense amyloid deposits (which are consistent with the observed increases in Aβ production), but no statistical differences in overall number or size of diffuse plaques or total plaque counts were observed in the older transgenic mice (18 weeks of age).

In a recent study, ABCA7 knock-out mice were crossed to the J20 APP transgenic model of amyloid pathology (12). In contrast to our findings, J20-ABCA7−/− mice had significantly increased insoluble Aβ at the late stage of pathology development (17 months) but no obvious differences in the soluble peptides. The different observations may be due to the characteristics of the particular APP transgenic mice under investigation. The TgCRND8 transgenic mice are an aggressive model of AD amyloid pathology with plaque development at 3–4 months as compared with the 15–17-month time frame for the J20 model. The fact that we did not observe substantial changes in the insoluble Aβ at 18 weeks in transgenic mouse models may be due to this rapid pace of pathology in the TgCRND8 mice that may potentially overwhelm clearance mechanisms.

Based on previous studies demonstrating significantly impaired phagocytosis in ABCA7 knock-out mice, it is quite feasible that ABCA7 does play a role in uptake and clearance of aggregated Aβ plaques and aggregates (14, 18, 46, 47). This would be consistent with several other genome-wide association study candidates that have been shown to regulate microglial activity necessary for amyloid removal as opposed to APP processing and trafficking. For example, CD33 is elevated in AD tissue and was found to inhibit macrophage uptake of Aβ in culture suggestive of impairments in phagocytosis (48). This was confirmed in CD33 knock-out mouse models crossed with APP transgenic mice that led to a substantial reduction in plaque density and levels of insoluble Aβ. In addition, a recently identified risk factor, TREM2, is linked to neuroinflammation and complement-related pathways and has been suggested to be involved in Aβ uptake (49, 50). However, our data indicate that ABCA7 also clearly has an impact on APP processing possibly through endocytosis-related pathways for which there are precedents with other AD at-risk genes.

SorLA (or Sorl1) for example is associated with LOAD, and changes in its expression have direct consequences for Aβ production (51). SorLA regulates intracellular trafficking of APP and when expressed at high levels, similar to ABCA7, reduces Aβ processing due to APP shuttling to endosomal and Golgi compartments (51, 52). SorLA-ablated mice when crossed to APP transgenic mice also have higher Aβ levels (53). Another LOAD-related gene, *PICALM*, has been shown in some (54, 55) but not other studies (56) to regulate APP processing and amyloid deposition in the opposite direction. PICALM overexpression *in vitro* was found to increase Aβ40 and Aβ42 through a preferential endocytosis of APP and the active form of the γ-secretase complex. Similar effects were found *in vivo* using virally mediated expression that led to elevated soluble and insoluble Aβ, whereas PICALM knockdown decreased both of these amyloid components (54).

A potential mechanism of action for ABCA7 can be envisioned along similar lines considering that ABCA7 co-localizes with LRP1 (18). It was observed that C1q-mediated enrichment of ABCA7 and LRP1 on the cell surface as well as membrane ruffles was markedly attenuated in hemizygous ABCA7+/− macrophages, and this was associated with decreased phagocytic activity as compared with wild-type cells (18). LRP1 is also one of the principal regulators of APP endocytosis and subsequent Aβ processing (for reviews, see Refs. 19 and 57). This is mediated by two phosphotyrosine binding domains in FE65 that interact with the NP*X*Y motifs within LRP1 and APP to effectively link the two proteins (58). The resulting LRP1-APP binding results in a more rapid endocytosis of APP and Aβ production (59, 60). It is therefore conceivable that disruptions in the ABCA7-LRP1 interaction lead to a dysregulation and enhancement of the LRP1-FE65-APP pathway to accelerate APP endocytosis that culminates in the observed increases in Aβ production in the ABCA7 knock-out mice. This would be consistent with the observed increase in APP endocytosis in the primary mouse microglia cells lacking ABCA7. Comparable changes in APP processing for a related family member, ABCA2, that result from alterations in the trafficking of γ-secretase components, particularly nicastrin, have been observed (61).

Studies to date have presented two potential mechanisms by which ABCA7 may contribute to AD pathology that involve Aβ production and/or clearance. Our current investigation supports an additional role for ABCA7 in APP processing leading to enhanced Aβ secretion, which may be linked to endocytosis activity. Although we did not observe the same extent of plaque accumulation in our APP transgenic mouse model as was seen in other studies (12), our findings support a role for ABCA7-mediated amyloid processing that may be working in combination with amyloid removal as factors for *ABCA7* at-risk allelic variants. Recent studies have led to the identification of multiple *ABCA7* coding variants that may also result in loss of function (62, 63). It will be of considerable interest to determine the effects of these ABCA7 mutants on APP processing and Aβ clearance. It is possible that ABCA7 may contribute to both pathways, and this study has focused on its impact on Aβ production. The role of ABCA7, if any, in Aβ removal is a key question and is the focus of separate future investigations.

Author Contributions—K. S. and P. E. F. coordinated the study and wrote the original version of the paper. K. S. acquired the data. K. S., S. A.-D., S. Y., P. S. G.-H., and P. E. F. made substantial contributions to the conception and design of the investigation as well as analysis and interpretation of the findings. All authors contributed to drafting the manuscript as well as revising it for clarity and intellectual contents.

Acknowledgments—We are very grateful for the supply of ABCA7 monoclonal antibody from Kyowa Hakko Kirin Co. Ltd. We also thank Rosemary Ahrens, Monika Duthie, Kathy Ha, and Kyung Han for invaluable technical assistance; Dr. Lili-Naz Hazrati for assistance with the amyloid immunohistochemistry; and Dr. Jennifer Griffin for assistance with primary cultures.

References

1. Hollingworth, P., Harold, D., Sims, R., Gerrish, A., Lambert, J.-C., Carrasquillo, M. M., Abraham, R., Hamshere, M. L., Pahwa, J. S., Moskvina, V., Dowzell, K., Jones, N., Stretton, A., Thomas, C., Richards, A., Ivanov, D., Widdowson, C., Chapman, J., Lovestone, S., Powell, J., Proitsi, P., Lupton, M. K., Brayne, C., Rubinsztein, D. C., Gill, M., Lawlor, B., Lynch, A., Brown, K. S., Passmore, P. A., Craig, D., McGuinness, B., Todd, S., Holmes, C., Mann, D., Smith, A. D., Beaumont, H., Warden, D., Wilcock, G., Love, S., Kehoe, P. G., Hooper, N. M., Vardy, E. R., Hardy, J., Mead, S., Fox, N. C., Rossor, M., Collinge, J., Maier, W., Jessen, F., Rüther, E., Schürmann, B., Heun, R., Kölsch, H., Van Den Bussche, H., Heuser, I., Kornhuber, J., Wiltfang, J., Dichgans, M., Frölich, L., Hampel, H., Gallacher, J., Hüll, M., Rujescu, D., Giegling, I., Goate, A. M., Kauwe, J. S., Cruchaga, C., Nowotny, P., Morris, J. C., Mayo, K., Sleegers, K., Bettens, K., Engelborghs, S., De Deyn, P. P., Van Broeckhoven, C., Livingston, G., Bass, N. J., Gurling, H., McQuillin, A., Gwilliam, R., Deloukas, P., Al-Chalabi, A., Shaw, C. E., Tsolaki, M., Singleton, A. B., Guerreiro, R., Mühleisen, T. W., Nöthen, M. M., Moebus, S., Jöckel, K.-H., Klopp, N., Wichmann, H.-E., Pankratz, V. S., Sando, S. B., Aasly, J. O., Barcikowska, M., Wszolek, Z. K., Dickson, D. W., Graff-Radford, N. R., Petersen, R. C., Van Duijn, C. M., Breteler, M. M., Ikram, M. A., Destefano, A. L., Fitzpatrick, A. L., Lopez, O., Launer, L. J., Seshadri, S., Berr, C., Campion, D., Epelbaum, J., Dartigues, J.-F., Tzourio, C., Alpérovitch, A., Lathrop, M., Feulner, T. M., Friedrich, P., Riehle, C., Krawczak, M., Schreiber, S., Mayhaus, M., Nicolhaus, S., Wagenpfeil, S., Steinberg, S., Stefansson, H., Stefansson, K., Snædal, J., Björnsson, S., Jonsson, P. V., Chouraki, V., Genier-Boley, B., Hiltunen, M., Soininen, H., Combarros, O., Zelenika, D., Delepine, M., Bullido, M. J., Pasquier, F., Mateo, I., Frank-Garcia, A., Porcellini, E., Hanon, O., Coto, E., Alvarez, V., Bosco, P., Siciliano, G., Mancuso, M., Panza, F., Solfrizzi, V., Nacmias, B., Sorbi, S., Bossù, P., Piccardi, P., Arosio, B., Annoni, G., Seripa, D., Pilotto, A., Scarpini, E., Galimberti, D., Brice, A., Hannequin, D., Licastro, F., Jones, L., Holmans, P. A., Jonsson, T., Riemenschneider, M., Morgan, K., Younkin, S. G., Owen, M. J., O'Donovan, M., Amouyel, P., and Williams, J. (2011) Common variants at *ABCA7*, *MS4A6A*/*MS4A4E*, *EPHA1*, *CD33* and *CD2AP* are associated with Alzheimer's disease. *Nat. Genet.* **43,** 429–435
2. Naj, A. C., Jun, G., Beecham, G. W., Wang, L.-S., Vardarajan, B. N., Buros, J., Gallins, P. J., Buxbaum, J. D., Jarvik, G. P., Crane, P. K., Larson, E. B., Bird, T. D., Boeve, B. F., Graff-Radford, N. R., De Jager, P. L., Evans, D., Schneider, J. A., Carrasquillo, M. M., Ertekin-Taner, N., Younkin, S. G., Cruchaga, C., Kauwe, J. S., Nowotny, P., Kramer, P., Hardy, J., Huentelman, M. J., Myers, A. J., Barmada, M. M., Demirci, F. Y., Baldwin, C. T., Green, R. C., Rogaeva, E., St George-Hyslop, P., Arnold, S. E., Barber, R., Beach, T., Bigio, E. H., Bowen, J. D., Boxer, A., Burke, J. R., Cairns, N. J., Carlson, C. S., Carney, R. M., Carroll, S. L., Chui, H. C., Clark, D. G., Corneveaux, J., Cotman, C. W., Cummings, J. L., DeCarli, C., DeKosky, S. T., Diaz-Arrastia, R., Dick, M., Dickson, D. W., Ellis, W. G., Faber, K. M., Fallon, K. B., Farlow, M. R., Ferris, S., Frosch, M. P., Galasko, D. R., Ganguli, M., Gearing, M., Geschwind, D. H., Ghetti, B., Gilbert, J. R., Gilman, S., Giordani, B., Glass, J. D., Growdon, J. H., Hamilton, R. L., Harrell, L. E., Head, E., Honig, L. S., Hulette, C. M., Hyman, B. T., Jicha, G. A., Jin, L.-W., Johnson, N., Karlawish, J., Karydas, A., Kaye, J. A., Kim, R., Koo, E. H., Kowall, N. W., Lah, J. J., Levey, A. I., Lieberman, A. P., Lopez, O. L., MacK, W. J., Marson, D. C., Martiniuk, F., Mash, D. C., Masliah, E., McCormick, W. C., McCurry, S. M., McDavid, A. N., McKee, A. C., Mesulam, M., Miller, B. L., Miller, C. A., Miller, J. W., Parisi, J. E., Perl, D. P., Peskind, E., Petersen, R. C., Poon, W. W., Quinn, J. F., Rajbhandary, R. A., Raskind, M., Reisberg, B., Ringman, J. M., Roberson, E. D., Rosenberg, R. N., Sano, M., Schneider, L. S., Seeley, W., Shelanski, M. L., Slifer, M. A., Smith, C. D., Sonnen, J. A., Spina, S., Stern, R. A., Tanzi, R. E., Trojanowski, J. Q., Troncoso, J. C., Van Deerlin, V. M., Vinters, H. V., Vonsattel, J. P., Weintraub, S., Welsh-Bohmer, K. A., Williamson, J., Woltjer, R. L., Cantwell, L. B., Dombroski, B. A., Beekly, D., Lunetta, K. L., Martin, E. R., Kamboh, M. I., Saykin, A. J., Reiman, E. M., Bennett, D. A., Morris, J. C., Montine, T. J., Goate, A. M., Blacker, D., Tsuang, D. W., Hakonarson, H., Kukull, W. A., Foroud, T. M., Haines, J. L., Mayeux, R., Pericak-Vance, M. A., Farrer, L. A., and Schellenberg, G. D. (2011) Common variants at *MS4A4*/*MS4A6E*, *CD2AP*, *CD33* and *EPHA1* are associated with late-onset Alzheimer's disease. *Nat. Genet.* **43,** 436–441
3. Reitz, C., Jun, G., Naj, A., Rajbhandary, R., Vardarajan, B. N., Wang, L.-S., Valladares, O., Lin, C.-F., Larson, E. B., Graff-Radford, N. R., Evans, D., De Jager, P. L., Crane, P. K., Buxbaum, J. D., Murrell, J. R., Raj, T., Ertekin-Taner, N., Logue, M., Baldwin, C. T., Green, R. C., Barnes, L. L., Cantwell, L. B., Fallin, M. D., Go, R. C., Griffith, P., Obisesan, T. O., Manly, J. J., Lunetta, K. L., Kamboh, M. I., Lopez, O. L., Bennett, D. A., Hendrie, H., Hall, K. S., Goate, A. M., Byrd, G. S., Kukull, W. A., Foroud, T. M., Haines, J. L., Farrer, L. A., Pericak-Vance, M. A., Schellenberg, G. D., Mayeux, R., and Alzheimer Disease Genetics Consortium (2013) Variants in the ATP-binding cassette transporter (ABCA7), apolipoprotein e ϵ4, and the risk of late-onset Alzheimer disease in African Americans. *JAMA* **309,** 1483–1492
4. Pohl, A., Devaux, P. F., and Herrmann, A. (2005) Function of prokaryotic and eukaryotic ABC proteins in lipid transport. *Biochim. Biophys. Acta* **1733,** 29–52
5. Wahrle, S. E., Jiang, H., Parsadanian, M., Hartman, R. E., Bales, K. R., Paul, S. M., and Holtzman, D. M. (2005) Deletion of Abca1 increases Aβ deposition in the PDAPP transgenic mouse model of Alzheimer disease. *J. Biol. Chem.* **280,** 43236–43242
6. Wahrle, S. E., Jiang, H., Parsadanian, M., Kim, J., Li, A., Knoten, A., Jain, S., Hirsch-Reinshagen, V., Wellington, C. L., Bales, K. R., Paul, S. M., and Holtzman, D. M. (2008) Overexpression of ABCA1 reduces amyloid deposition in the PDAPP mouse model of Alzheimer disease. *J. Clin. Investig.* **118,** 671–682
7. Koldamova, R., Staufenbiel, M., and Lefterov, I. (2005) Lack of ABCA1 considerably decreases brain ApoE level and increases amyloid deposition in APP23 mice. *J. Biol. Chem.* **280,** 43224–43235
8. Chan, S. L., Kim, W. S., Kwok, J. B., Hill, A. F., Cappai, R., Rye, K.-A., and Garner, B. (2008) ATP-binding cassette transporter A7 regulates processing of amyloid precursor protein in vitro. *J. Neurochem.* **106,** 793–804
9. Abe-Dohmae, S., Ikeda, Y., Matsuo, M., Hayashi, M., Okuhira, K., Ueda, K., and Yokoyama, S. (2004) Human ABCA7 supports apolipoprotein-mediated release of cellular cholesterol and phospholipid to generate high density lipoprotein. *J. Biol. Chem.* **279,** 604–611
10. Hayashi, M., Abe-Dohmae, S., Okazaki, M., Ueda, K., and Yokoyama, S. (2005) Heterogeneity of high density lipoprotein generated by ABCA1 and ABCA7. *J. Lipid Res.* **46,** 1703–1711
11. Wang, N., Lan, D., Gerbod-Giannone, M., Linsel-Nitschke, P., Jehle, A. W., Chen, W., Martinez, L. O., and Tall, A. R. (2003) ATP-binding cassette transporter A7 (ABCA7) binds apolipoprotein A-I and mediates cellular phospholipid but not cholesterol efflux. *J. Biol. Chem.* **278,** 42906–42912
12. Kim, W. S., Li, H., Ruberu, K., Chan, S., Elliott, D. A., Low, J. K., Cheng, D., Karl, T., and Garner, B. (2013) Deletion of Abca7 increases cerebral amyloid-β accumulation in the J20 mouse model of Alzheimer's disease. *J. Neurosci.* **33,** 4387–4394
13. Linsel-Nitschke, P., Jehle, A. W., Shan, J., Cao, G., Bacic, D., Lan, D., Wang, N., and Tall, A. R. (2005) Potential role of ABCA7 in cellular lipid efflux to apoA-I. *J. Lipid Res.* **46,** 86–92
14. Iwamoto, N., Abe-Dohmae, S., Sato, R., and Yokoyama, S. (2006) ABCA7 expression is regulated by cellular cholesterol through the SREBP2 pathway and associated with phagocytosis. *J. Lipid Res.* **47,** 1915–1927
15. Tanaka, N., Abe-Dohmae, S., Iwamoto, N., and Yokoyama, S. (2011) Roles of ATP-binding cassette transporter A7 in cholesterol homeostasis and host defense system. *J. Atheroscler. Thromb.* **18,** 274–281
16. Abe-Dohmae, S., and Yokoyama, S. (2012) ABCA7: a potential mediator between cholesterol homeostasis and the host defense system. *Clin. Lipidol.* **7,** 677–687
17. Soscia, S. J., and Fitzgerald, M. L. (2013) The ABCA7 transporter, brain lipids and Alzheimer's disease. *Clin. Lipidol.* **8,** 97–108
18. Jehle, A. W., Gardai, S. J., Li, S., Linsel-Nitschke, P., Morimoto, K., Janssen, W. J., Vandivier, R. W., Wang, N., Greenberg, S., Dale, B. M., Qin, C., Henson, P. M., and Tall, A. R. (2006) ATP-binding cassette transporter A7 enhances phagocytosis of apoptotic cells and associated ERK signaling in macrophages. *J. Cell Biol.* **174,** 547–556
19. Jaeger, S., and Pietrzik, C. U. (2008) Functional role of lipoprotein recep-

tors in Alzheimer's disease. *Curr. Alzheimer Res.* **5,** 15–25
20. Bu, G., Cam, J., and Zerbinatti, C. (2006) LRP in amyloid-β production and metabolism. *Ann. N.Y. Acad. Sci.* **1086,** 35–53
21. Tanaka, A. R., Ikeda, Y., Abe-Dohmae, S., Arakawa, R., Sadanami, K., Kidera, A., Nakagawa, S., Nagase, T., Aoki, R., Kioka, N., Amachi, T., Yokoyama, S., and Ueda, K. (2001) Human ABCA1 contains a large amino-terminal extracellular domain homologous to an epitope of Sjögren's Syndrome. *Biochem. Biophys. Res. Commun.* **283,** 1019–1025
22. Cole, R., and de Vellis, J. (2001) in *Protocols for Neural Cell Culture* (Fedoroff, S., and Richardson, A., eds) 3rd Ed., pp. 117–127, Humana Press, Totowa, NJ
23. Hertz, L., Juurlink, B. H. J., Fosmark, H., and Schousboe, A. (1982) in *Neuroscience Approached Through Cell Culture* (Pfeiffer, S. E., ed) Vol. 1, pp. 175–186, CRC Press Boca Raton, FL
24. Zhou, Y., Li, H. L., Zhao, R., Yang, L. T., Dong, Y., Yue, X., Ma, Y. Y., Wang, Z., Chen, J., Cui, C. L., and Yu, A. C. (2010) Astrocytes express N-methyl-D-aspartate receptor subunits in development, ischemia and post-ischemia. *Neurochem. Res.* **35,** 2124–2134
25. Saura, J., Tusell, J. M., and Serratosa, J. (2003) High-yield isolation of murine microglia by mild trypsinization. *GLIA* **44,** 183–189
26. Jiang, Y., Mullaney, K. A., Peterhoff, C. M., Che, S., Schmidt, S. D., Boyer-Boiteau, A., Ginsberg, S. D., Cataldo, A. M., Mathews, P. M., and Nixon, R. A. (2010) Alzheimer's-related endosome dysfunction in Down syndrome is Aβ-independent but requires APP and is reversed by BACE-1 inhibition. *Proc. Natl. Acad. Sci. U.S.A.* **107,** 1630–1635
27. Chishti, M. A., Yang, D.-S., Janus, C., Phinney, A. L., Horne, P., Pearson, J., Strome, R., Zuker, N., Loukides, J., French, J., Turner, S., Lozza, G., Grilli, M., Kunicki, S., Morissette, C., Paquette, J., Gervais, F., Bergeron, C., Fraser, P. E., Carlson, G. A., St George-Hyslop, P., and Westaway, D. (2001) Early-onset amyloid deposition and cognitive deficits in transgenic mice expressing a double mutant form of amyloid precursor protein 695. *J. Biol. Chem.* **276,** 21562–21570
28. Kim, W. S., Fitzgerald, M. L., Kang, K., Okuhira, K., Bell, S. A., Manning, J. J., Koehn, S. L., Lu, N., Moore, K. J., and Freeman, M. W. (2005) ABCA7 null mice retain normal macrophage phosphatidylcholine and cholesterol efflux activity despite alterations in adipose mass and serum cholesterol levels. *J. Biol. Chem.* **280,** 3989–3995
29. Janus, C., Pearson, J., McLaurin, J., Mathews, P. M., Jiang, Y., Schmidt, S. D., Chishti, M. A., Horne, P., Heslin, D., French, J., Mount, H. T., Nixon, R. A., Mercken, M., Bergeron, C., Fraser, P. E., St George-Hyslop, P., and Westaway, D. (2000) Aβ peptide immunization reduces behavioural impairment and plaques in a model of Alzheimer's disease. *Nature* **408,** 979–982
30. Bachstetter, A. D., Norris, C. M., Sompol, P., Wilcock, D. M., Goulding, D., Neltner, J. H., St Clair, D., Watterson, D. M., and Van Eldik, L. J. (2012) Early stage drug treatment that normalizes proinflammatory cytokine production attenuates synaptic dysfunction in a mouse model that exhibits age-dependent progression of Alzheimer's disease-related pathology. *J. Neurosci.* **32,** 10201–10210
31. Durk, M. R., Han, K., Chow, E. C., Ahrens, R., Henderson, J. T., Fraser, P. E., and Pang, K. S. (2014) 1α,25-Dihydroxyvitamin D3 reduces cerebral amyloid-β accumulation and improves cognition in mouse models of Alzheimer's disease. *J. Neurosci.* **34,** 7091–7101
32. Walter, J. (2012) γ-Secretase, apolipoprotein E and cellular cholesterol metabolism. *Curr. Alzheimer Res.* **9,** 189–199
33. Tremblay, P., Bouzamondo-Bernstein, E., Heinrich, C., Prusiner, S. B., and DeArmond, S. J. (2007) Developmental expression of PrP in the post-implantation embryo. *Brain Res.* **1139,** 60–67
34. Kinoshita, A., Fukumoto, H., Shah, T., Whelan, C. M., Irizarry, M. C., and Hyman, B. T. (2003) Demonstration by FRET of BACE interaction with the amyloid precursor protein at the cell surface and in early endosomes. *J. Cell Sci.* **116,** 3339–3346
35. Steinberg, S., Stefansson, H., Jonsson, T., Johannsdottir, H., Ingason, A., Helgason, H., Sulem, P., Magnusson, O. T., Gudjonsson, S. A., Unnsteinsdottir, U., Kong, A., Helisalmi, S., Soininen, H., Lah, J. J., DemGene, Aarsland, D., Fladby, T., Ulstein, I. D., Djurovic, S., Sando, S. B., White, L. R., Knudsen, G.-P., Westlye, L. T., Selbæk, G., Giegling, I., Hampel, H., Hiltunen, M., Levey, A. I., Andreassen, O. A., Rujescu, D., Jonsson, P. V., Bjornsson, S., Snaedal, J., and Stefansson, K. (2015) Loss-of-function variants in *ABCA7* confer risk of Alzheimer's disease. *Nat. Genet.* **47,** 445–447
36. Yu, L., Chibnik, L. B., Srivastava, G. P., Pochet, N., Yang, J., Xu, J., Kozubek, J., Obholzer, N., Leurgans, S. E., Schneider, J. A., Meissner, A., De Jager, P. L., and Bennett, D. A. (2015) Association of brain DNA methylation in *SORL1*, *ABCA7*, *HLA-DRB5*, *SLC24A4*, and *BIN1* with pathological diagnosis of Alzheimer disease. *JAMA Neurol.* **72,** 15–24
37. Bali, J., Gheinani, A. H., Zurbriggen, S., and Rajendran, L. (2012) Role of genes linked to sporadic Alzheimer's disease risk in the production of β-amyloid peptides. *Proc. Natl. Acad. Sci. U.S.A.* **109,** 15307–15311
38. Logge, W., Cheng, D., Chesworth, R., Bhatia, S., Garner, B., Kim, W. S., and Karl, T. (2012) Role of Abca7 in mouse behaviours relevant to neurodegenerative diseases. *PLoS One* **7,** e45959
39. Lue, L. F., Kuo, Y. M., Roher, A. E., Brachova, L., Shen, Y., Sue, L., Beach, T., Kurth, J. H., Rydel, R. E., and Rogers, J. (1999) Soluble amyloid β peptide concentration as a predictor of synaptic change in Alzheimer's disease. *Am. J. Pathol.* **155,** 853–862
40. Klein, W. L., Krafft, G. A., and Finch, C. E. (2001) Targeting small Aβ oligomers: the solution to an Alzheimer's disease conundrum? *Trends Neurosci.* **24,** 219–224
41. Selkoe, D. J. (2002) Alzheimer's disease is a synaptic failure. *Science* **298,** 789–791
42. Gong, Y., Chang, L., Viola, K. L., Lacor, P. N., Lambert, M. P., Finch, C. E., Krafft, G. A., and Klein, W. L. (2003) Alzheimer's disease-affected brain: presence of oligomeric Aβ ligands (ADDLs) suggests a molecular basis for reversible memory loss. *Proc. Natl. Acad. Sci. U.S.A.* **100,** 10417–10422
43. Lesné, S., Koh, M. T., Kotilinek, L., Kayed, R., Glabe, C. G., Yang, A., Gallagher, M., and Ashe, K. H. (2006) A specific amyloid-β protein assembly in the brain impairs memory. *Nature* **440,** 352–357
44. Lacor, P. N., Buniel, M. C., Furlow, P. W., Clemente, A. S., Velasco, P. T., Wood, M., Viola, K. L., and Klein, W. L. (2007) Aβ oligomer-induced aberrations in synapse composition, shape, and density provide a molecular basis for loss of connectivity in Alzheimer's disease. *J. Neurosci.* **27,** 796–807
45. Tomiyama, T., Matsuyama, S., Iso, H., Umeda, T., Takuma, H., Ohnishi, K., Ishibashi, K., Teraoka, R., Sakama, N., Yamashita, T., Nishitsuji, K., Ito, K., Shimada, H., Lambert, M. P., Klein, W. L., and Mori, H. (2010) A mouse model of amyloid β oligomers: their contribution to synaptic alteration, abnormal tau phosphorylation, glial activation, and neuronal loss *in vivo*. *J. Neurosci.* **30,** 4845–4856
46. Tanaka, N., Abe-Dohmae, S., Iwamoto, N., Fitzgerald, M. L., and Yokoyama, S. (2010) Helical apolipoproteins of high-density lipoprotein enhance phagocytosis by stabilizing ATP-binding cassette transporter A7. *J. Lipid Res.* **51,** 2591–2599
47. Tanaka, N., Abe-Dohmae, S., Iwamoto, N., Fitzgerald, M. L., and Yokoyama, S. (2011) HMG-CoA reductase inhibitors enhance phagocytosis by upregulating ATP-binding cassette transporter A7. *Atherosclerosis* **217,** 407–414
48. Griciuc, A., Serrano-Pozo, A., Parrado, A. R., Lesinski, A. N., Asselin, C. N., Mullin, K., Hooli, B., Choi, S. H., Hyman, B. T., and Tanzi, R. E. (2013) Alzheimer's disease risk gene CD33 inhibits microglial uptake of amyloid β. *Neuron* **78,** 631–643
49. Guerreiro, R., Wojtas, A., Bras, J., Carrasquillo, M., Rogaeva, E., Majounie, E., Cruchaga, C., Sassi, C., Kauwe, J. S., Younkin, S., Hazrati, L., Collinge, J., Pocock, J., Lashley, T., Williams, J., Lambert, J. C., Amouyel, P., Goate, A., Rademakers, R., Morgan, K., Powell, J., St George-Hyslop, P., Singleton, A., Hardy, J., and Alzheimer Genetic Analysis Group (2013) TREM2 variants in Alzheimer's disease. *New Engl. J. Med.* **368,** 117–127
50. Jonsson, T., Stefansson, H., Steinberg, S., Jonsdottir, I., Jonsson, P. V., Snaedal, J., Bjornsson, S., Huttenlocher, J., Levey, A. I., Lah, J. J., Rujescu, D., Hampel, H., Giegling, I., Andreassen, O. A., Engedal, K., Ulstein, I., Djurovic, S., Ibrahim-Verbaas, C., Hofman, A., Ikram, M. A., van Duijn, C. M., Thorsteinsdottir, U., Kong, A., and Stefansson, K. (2013) Variant of TREM2 associated with the risk of Alzheimer's disease. *New Eng. J. Med.* **368,** 107–116
51. Rogaeva, E., Meng, Y., Lee, J. H., Gu, Y., Kawarai, T., Zou, F., Katayama, T., Baldwin, C. T., Cheng, R., Hasegawa, H., Chen, F., Shibata, N., Lunetta, K. L., Pardossi-Piquard, R., Bohm, C., Wakutani, Y., Cupples, L. A.,

Cuenco, K. T., Green, R. C., Pinessi, L., Rainero, I., Sorbi, S., Bruni, A., Duara, R., Friedland, R. P., Inzelberg, R., Hampe, W., Bujo, H., Song, Y. Q., Andersen, O. M., Willnow, T. E., Graff-Radford, N., Petersen, R. C., Dickson, D., Der, S. D., Fraser, P. E., Schmitt-Ulms, G., Younkin, S., Mayeux, R., Farrer, L. A., and St George-Hyslop, P. (2007) The neuronal sortilin-related receptor SORL1 is genetically associated with Alzheimer disease. *Nat. Genet.* **39,** 168–177

52. Andersen, O. M., Reiche, J., Schmidt, V., Gotthardt, M., Spoelgen, R., Behlke, J., von Arnim, C. A., Breiderhoff, T., Jansen, P., Wu, X., Bales, K. R., Cappai, R., Masters, C. L., Gliemann, J., Mufson, E. J., Hyman, B. T., Paul, S. M., Nykjaer, A., and Willnow, T. E. (2005) Neuronal sorting protein-related receptor sorLA/LR11 regulates processing of the amyloid precursor protein. *Proc. Natl. Acad. Sci. U.S.A.* **102,** 13461–13466
53. Dodson, S. E., Andersen, O. M., Karmali, V., Fritz, J. J., Cheng, D., Peng, J., Levey, A. I., Willnow, T. E., and Lah, J. J. (2008) Loss of LR11/SORLA enhances early pathology in a mouse model of amyloidosis: evidence for a proximal role in Alzheimer's disease. *J. Neurosci.* **28,** 12877–12886
54. Xiao, Q., Gil, S.-C., Yan, P., Wang, Y., Han, S., Gonzales, E., Perez, R., Cirrito, J. R., and Lee, J.-M. (2012) Role of phosphatidylinositol clathrin assembly lymphoid-myeloid leukemia (PICALM) in intracellular amyloid precursor protein (APP) processing and amyloid plaque pathogenesis. *J. Biol. Chem.* **287,** 21279–21289
55. Kanatsu, K., Morohashi, Y., Suzuki, M., Kuroda, H., Watanabe, T., Tomita, T., and Iwatsubo, T. (2014) Decreased CALM expression reduces Aβ42 to total Aβ ratio through clathrin-mediated endocytosis of γ-secretase. *Nat. Commun.* **5,** 3386
56. Wu, F., Matsuoka, Y., Mattson, M. P., and Yao, P. J. (2009) The clathrin assembly protein AP180 regulates the generation of amyloid-β peptide. *Biochem. Biophys. Res. Commun.* **385,** 247–250
57. Bu, G. (2009) Apolipoprotein E and its receptors in Alzheimer's disease: pathways, pathogenesis and therapy. *Nat. Rev. Neurosci.* **10,** 333–344
58. Pietrzik, C. U., Yoon, I.-S., Jaeger, S., Busse, T., Weggen, S., and Koo, E. H. (2004) FE65 constitutes the functional link between the low-density lipoprotein receptor related protein and the amyloid precursor protein. *J. Neurosci.* **24,** 4259–4265
59. Ulery, P. G., Beers, J., Mikhailenko, I., Tanzi, R. E., Rebeck, G. W., Hyman, B. T., and Strickland, D. K. (2000) Modulation of β-amyloid precursor protein processing by the low density lipoprotein receptor-related protein (LRP) Evidence that LRP contributes to the pathogenesis of Alzheimer's disease. *J. Biol. Chem.* **275,** 7410–7415
60. Cam, J. A., Zerbinatti, C. V., Li, Y., and Bu, G. (2005) Rapid endocytosis of the low density lipoprotein receptor related protein modulates cell surface distribution and processing of the β-amyloid precursor protein. *J. Biol. Chem.* **280,** 15464–15470
61. Michaki, V., Guix, F. X., Vennekens, K., Munck, S., Dingwall, C., Davis, J. B., Townsend, D. M., Tew, K. D., Feiguin, F., De Strooper, B., Dotti, C. G., and Wahle, T. (2012) Down-regulation of the ATP-binding cassette transporter 2 (Abca2) reduces amyloid-β production by altering nicastrin maturation and intracellular localization. *J. Biol. Chem.* **287,** 1100–1111
62. Ghani, M., Lang, A. E., Zinman, L., Nacmias, B., Sorbi, S., Bessi, V., Tedde, A., Tartaglia, M. C., Surace, E. I., Sato, C., Moreno, D., Xi, Z., Hung, R., Nalls, M. A., Singleton, A., St George-Hyslop, P., and Rogaeva, E. (2015) Mutation analysis of patients with neurodegenerative disorders using NeuroX array. *Neurobiol. Aging* **36,** 545.e9–545.e14
63. Cuyvers, E., De Roeck, A., Van den Bossche, T., Van Cauwenberghe, C., Bettens, K., Vermeulen, S., Mattheijssens, M., Peeters, K., Engelborghs, S., Vandenbulcke, M., Vandenberghe, R., De Deyn, P. P., Van Broeckhoven, C., and Sleegers, K. (2015) Mutations in *ABCA7* in a Belgian cohort of Alzheimer's disease patients: a targeted resequencing study. *Lancet Neurol.* **14,** 814–822
64. Bradford, M. M. (1976) A rapid and sensitive method for the quantitation of microgram quantities of protein utilizing the principle of protein-dye binding. *Anal. Biochem.* **72,** 248–254